Ceramics International **23** (1997) 413–418

PII: S0272-8842(96)00048-X
0272-8842/97 $17.00 + 0.00

Microstructural Mechanisms of Cyclic Fatigue-Crack Propagation in Grain-Bridging Ceramics*

C. J. Gilbert,[a] R. H. Dauskardt[b] & R. O. Ritchie[a]

[a]Department of Materials Science and Mineral Engineering, University of California, Berkeley, CA 94720-1760, USA
[b]Department of Materials Science and Engineering, Stanford University, Stanford, CA 94305-2205, USA

(Received 30 June 1995; accepted 17 January 1996)

Abstract: The microstructural basis of cyclic fatigue-crack propagation in grain-bridging ceramics is investigated for monolithic, hot-pressed alumina and silicon nitride. In both materials, rates of subcritical crack growth under cyclic loads are observed to be many orders of magnitude faster than corresponding growth rates under monotonic loading at equivalent stress-intensity levels. This behaviour is attributed to diminished crack-tip shielding under cyclic loads caused by a degradation of the grain-bridging zone in the wake of the crack tip associated with frictional wear at the grain/matrix interface: the reduced shielding acts locally to enhance the crack-tip driving force in cyclic fatigue. Micromechanical modelling of this process is shown to be consistent with fractographic and *in situ* crack-profile analyses. The effect on crack-growth rates of microstructural and mechanical variables are examined in light of this mechanism. © 1997 Elsevier Science Limited and Techna S.r.l.

1 INTRODUCTION

Despite advances in the toughening of structural ceramics, little is understood about their degradation under cyclic loading. While limited fatigue data have been collected in several systems, few studies have focused on a systematic characterization of the effects of microstructural and mechanical variables. More importantly, microstructural factors governing cyclic crack advance remain largely undocumented. Recent modelling[1,2] has shown that sliding wear of frictional grain bridges under cyclic loading can result in premature debonding of grains and reduced pullout stresses, factors which reduce the toughening capacity of grain-bridging ceramics; similar mechanisms are apparent in whisker or fibre composites. Such models permit calculation of fatigue-crack growth rate behaviour for ceramics and predict growth rates to be markedly sensitive to the applied stress intensity and to microstructural and mechanical parameters such as grain size and load ratio. It is therefore the focus of the present study to characterize cyclic fatigue-crack growth behaviour in several grades of Al_2O_3 and in a Si_3N_4 in light of these models, and to elucidate dominant microstructural mechanisms for crack advance.

2 EXPERIMENTAL PROCEDURES

Five grades of monolithic Al_2O_3 were examined, namely two Coors materials, one with a purity of 99.5%, a bimodal grain size distribution, and a fracture toughness $K_c \sim 5.3$ MPa$\sqrt{m}$, the other with a purity of 95.5%, a non-uniform grain size distribution, and a $K_c \sim 5.3$ MPa$\sqrt{m}$, and three grades processed by isostatically pressing high-purity Al_2O_3 powders at 1700 °C *in vacuo*. The latter three microstructures (with equiaxed grain sizes of 8 μm, 10 μm and 13 μm) displayed significant resistance-curve behaviour, with crack initiation values of ~ 2.5 MPa$\sqrt{m}$ and steady-state K_c values

*Proc. 8th CIMTEC, World Ceramics Congress and Forum on New Materials, Florence, Italy.

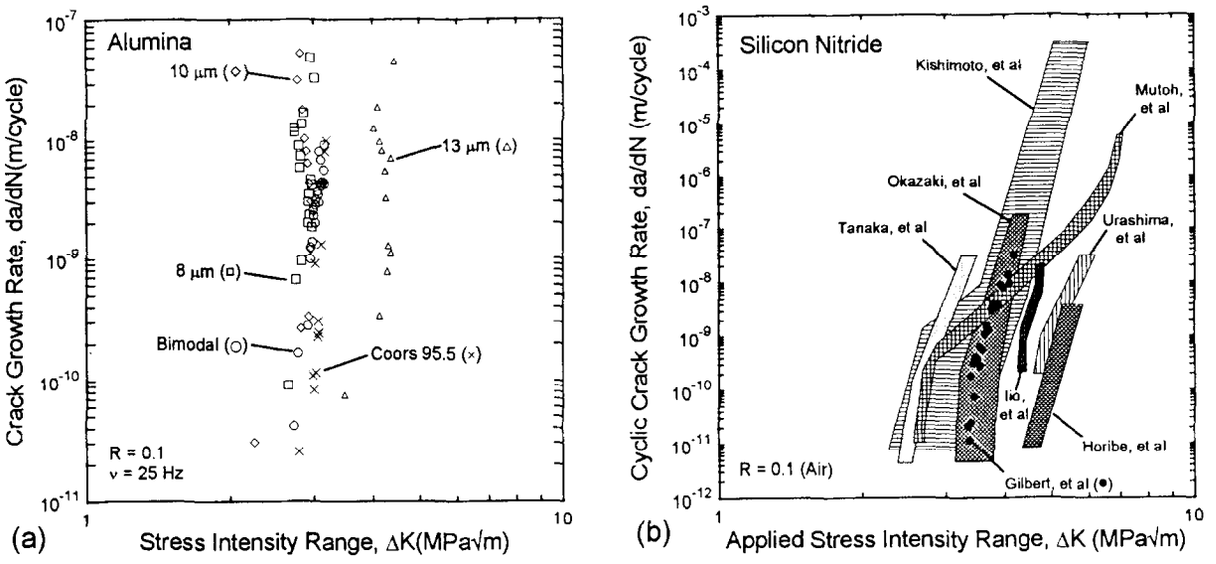

Fig. 1. Fatigue-crack growth rate data for the Al_2O_3 and Si_3N_4.

of 3.7 MPa$\sqrt{m}$, 4.4 MPa$\sqrt{m}$ and 5.3 MPa$\sqrt{m}$, respectively. In addition, tests were performed on an NTK Technical Ceramics Si_3N_4 (designation EC-141); this material also displayed significant R-curve behaviour, with a steady-state fracture toughness of $K_c \sim 5.8$ MPa$\sqrt{m}$. Microstructures and mechanical properties have been reported elsewhere.[3,4]

Cyclic crack-growth rate measurements were performed in a controlled room-air environment (22 °C, 45% relative humidity) at a frequency $\mp < \nabla\zeta\ \alpha\nu\delta\ \lambda\omega\alpha\delta\ \rho\alpha\tau\iota\omega\sigma\cdot\cdot$ $R = K_{min}/K_{max}$, of 0.1, 0.5 and 0.7 using compact-tension C(T) and disk-shaped compact-tension DC(T) specimens. Test methods are described elsewhere.[5] Fracture surfaces were examined in the scanning electron microscope (SEM), and crack profiles in the SEM using an *in situ* miniature screw-driven loading stage.

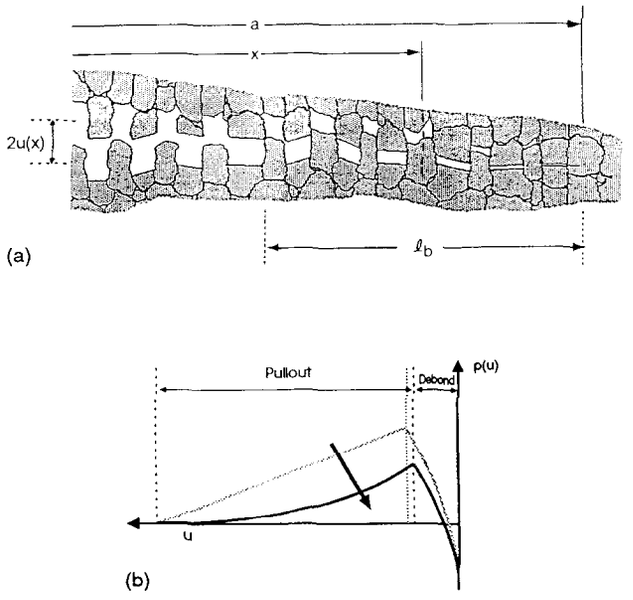

Fig. 2. Schematic of grain bridges in the wake of a growing crack. The grain bridging stress, $p(u)$, is shown to decrease with cycling. After Ref. 1.

3 RESULTS AND DISCUSSION

Both materials display accelerated growth rates under cyclic loading, as shown by comparing crack velocities at a constant applied stress intensity, K_{max}, to those measured under cyclic loading with the same K_{max}. Cyclic fatigue-crack growth rate data are plotted over four orders of magnitude ($R = 0.1$, $\nu = 25$ Hz) in Fig. 1(a) for all five Al_2O_3 microstructures, and in Fig. 1(b) for Si_3N_4; results are seen to compare well with literature values.[6,7] Similar to metallic materials over the mid-range of growth rates, these data may be expressed in terms of a simple Paris-law relationship of the form $da/dN = C\Delta K^m$, where C and m are scaling constants. The exponents, m, are far higher in the ceramics ($m \sim 16$ to 47 for Al_2O_3, and $m \sim 30$ for Si_3N_4) than those reported for metallic systems, where m typically lies between 2 and 4. For the equiaxed aluminas, growth rates are seen to increase, and fatigue thresholds to decrease, with both decreasing grain size and decreasing toughness, K_c; behaviour can be normalized, however, by plotting as a function of K_{max}/K_c.[3]

Such fatigue behaviour can be modelled in terms of a reduction in the grain-bridging stress function, $p(u)$, which characterizes crack-surface closing tractions developed in the bridging zone (Fig. 2)[1] ($2u$ represents crack-opening displacement). During grain debonding, $p(u)$ rises steeply from an

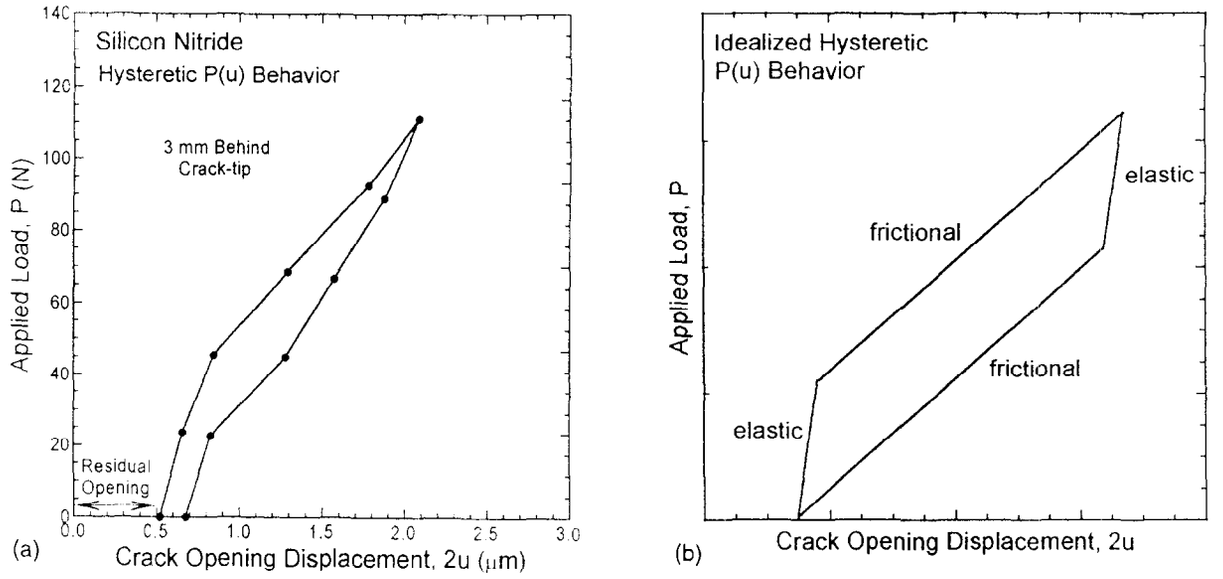

Fig. 3. Hysteretic behaviour in Si_3N_4. Such behaviour is idealized in (b).

initial compressive residual stress, σ_R, to a maximum tensile value representing detachment of the bridge from the matrix. This increase is followed by a gradual decrease dominated by frictional pullout, generally represented by a relationship of the form[1] $p(u) = \mu\sigma_N (1 - u/u^*)$, where μ is the frictional coefficient and σ_N the normal stress acting on the bridge/matrix boundary ($\sigma_N = \sigma_R$). The critical crack-opening displacement at bridge rupture (typically half the grain size) is represented by u^*. A measure of the energy dissipated during pullout is given by the area under $p(u)$; initial debonding, which consumes far less energy, is ignored. The resultant increase in toughness, G_b (the toughening capacity of the bridging zone), is determined using energy balance arguments,[8] and the near-tip driving force, G_{tip}, is given by $G_{tip} = G_{app} - G_b$, where G_{app} represents the applied level of far-field loading. Accumulated wear damage at the bridge/matrix interface[1,2] results in a reduction in the toughening capacity of the bridging zone, G_b, under cyclic loads, leading to an increase in the crack-tip driving force, G_{tip}.

Such analyses were found to be consistent with *in situ* SEM observations of fatigue crack profiles. Hysteresis was observed in plots of $2u$ vs load, P, in both materials (e.g. Si_3N_4 in Fig. 3(a)). Upon initial loading, bridges behave elastically until loads are sufficient to overcome frictional resistance, at which point the compliance is reduced below the elastic value. With subsequent unloading, the bridges relax elastically, followed by frictional sliding as they return to their initial positions (Fig. 3(b)). The area under this curve reflects irreversible energy loss per loading cycle, which is related to the shielding capacity of the bridging zone, G_b.[9]

Observation of bridging sites in the 13 μm grain-sized alumina suggest that this energy dissipation results from elimination of the shielding capacity of bridging grains under cycling. Figure 4(a) shows the same grain as Fig. 4(b) prior to the application of $\sim 2\times10^6$ loading cycles. There is evidence of damage to the bridge; moreover, the secondary crack (indicated by the arrow) has closed relative to its position in Fig. 4(a), presumably because of a reduction in local frictional tractions. In addition, wear damage seen on cyclic fatigue fracture surfaces is consistent with a reduction in the potency of grain-bridging phenomenon under cyclic loads (Fig. 5).

Lathabai *et al.*[2] has modelled the reduction of the bridging capacity in terms of a decrease in the frictional coefficient μ at the grain/matrix interface. The necessary reduction in μ is obtained by fitting the model to experimental stress-life data. Alterna-

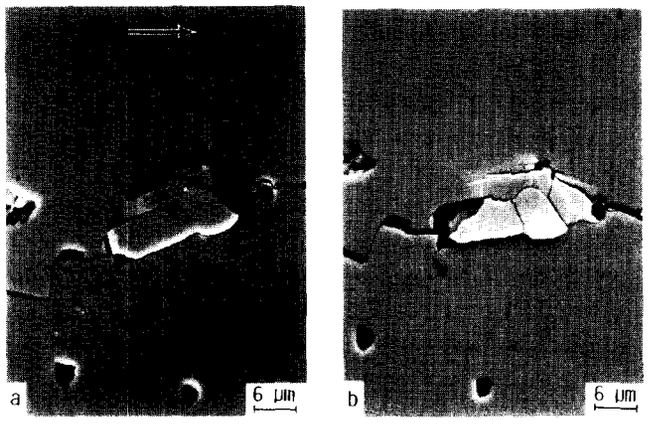

Fig. 4. Bridge in the 13 μm grain-sized Al_2O_3 (a) before and (b) after ~2 million cycles.

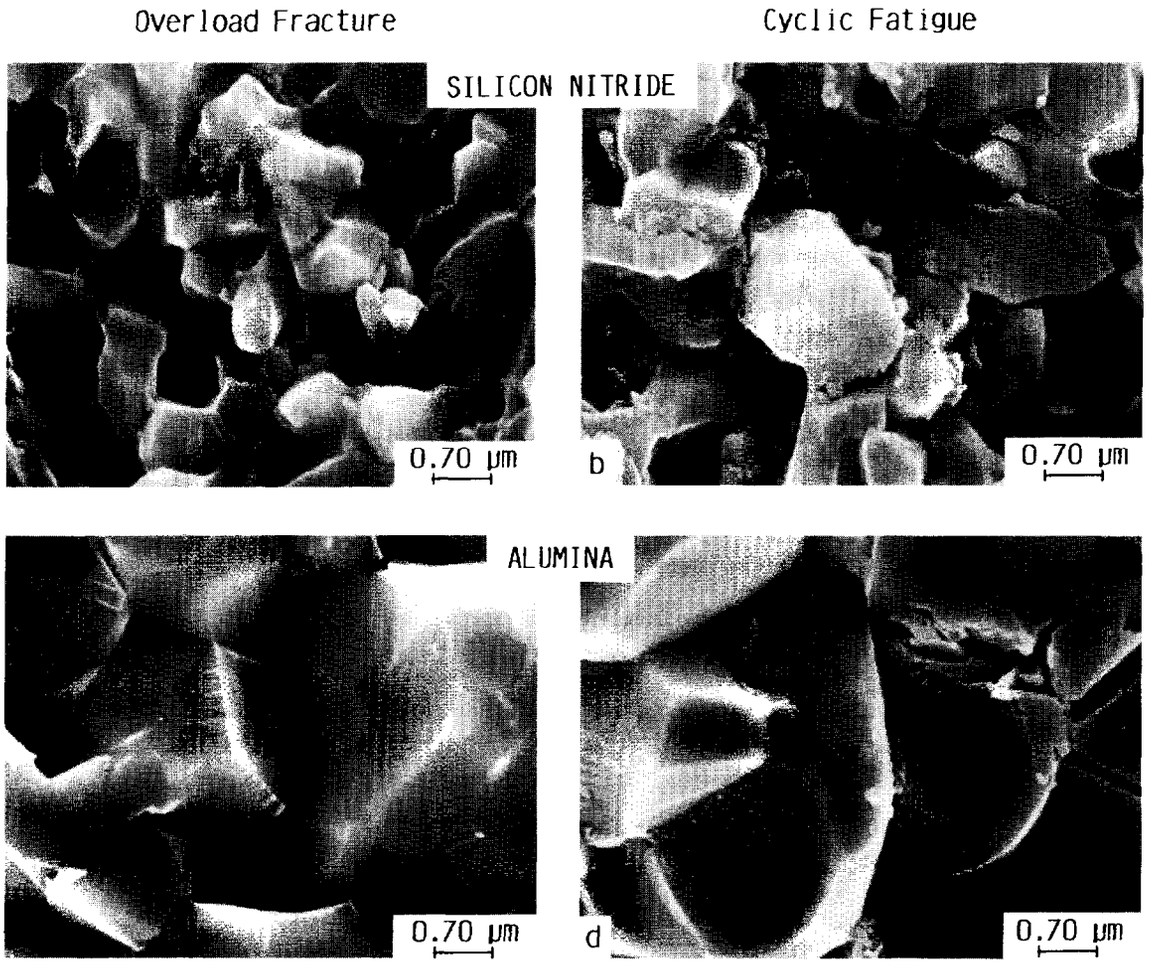

Fig. 5. Fracture surfaces in (a), (b) Si_3N_4 and (c), (d) the 13 μm grain-sized Al_2O_3.

tively, the degradation in $p(u)$ can be modelled in terms of the effect of material removed from the bridge/matrix interface by sliding wear processes on the residual stress, σ_R, induced by thermal expansion anisotropy (TEA).[1] Using the results of Eshelby,[10] the normal stress, σ_N, acting across the sliding interface is taken to be σ_R, and is directly related to ϵ_r, the radial misfit strain arising from TEA. Wear at the grain/matrix interface is simulated by adjusting ϵ_r to accommodate material being removed from the interface during cycling, and is quantified using a simple wear relationship (based on Amonton's Law) in terms of the normal stress at the interface and the sliding distance.[1]

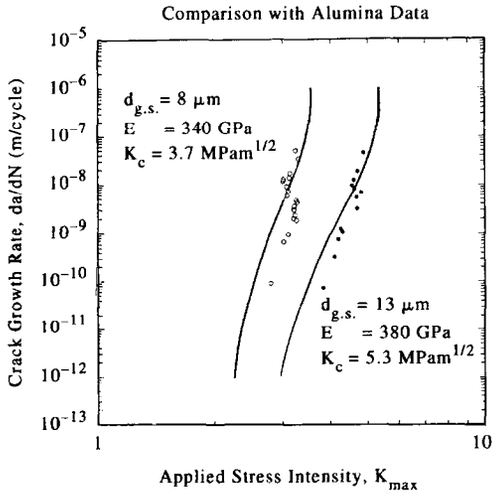

Fig. 6. Comparisons between predicted and measured crack-growth rates in Al_2O_3.

By relating the amount of material removed at the grain/matrix interface to ϵ_r, σ_R and the frictional pullout function $p(u)$, where $\sigma_N = \sigma_R$, the decrease in the shielding capacity of the zone can be calculated. Based on such a calculation, the near-tip driving force, K_{tip}, is determined, thereby providing a condition for steady-state crack growth at constant da/dN of the form $K_{tip} = K_0$, where K_0 is the intrinsic matrix toughness.

Growth rates in the three equiaxed aluminas are seen to increase with decreasing grain size (Fig. 1(a)), consistent with such a bridging/degradation model. This effect is associated primarily with the enhanced toughness found in coarser microstructures, consistent with the successful normalization of growth rate data when plotted in terms of K_{max}/K_c.[3] It is significant to note that predictions correlate well with experimental data (Fig. 6).

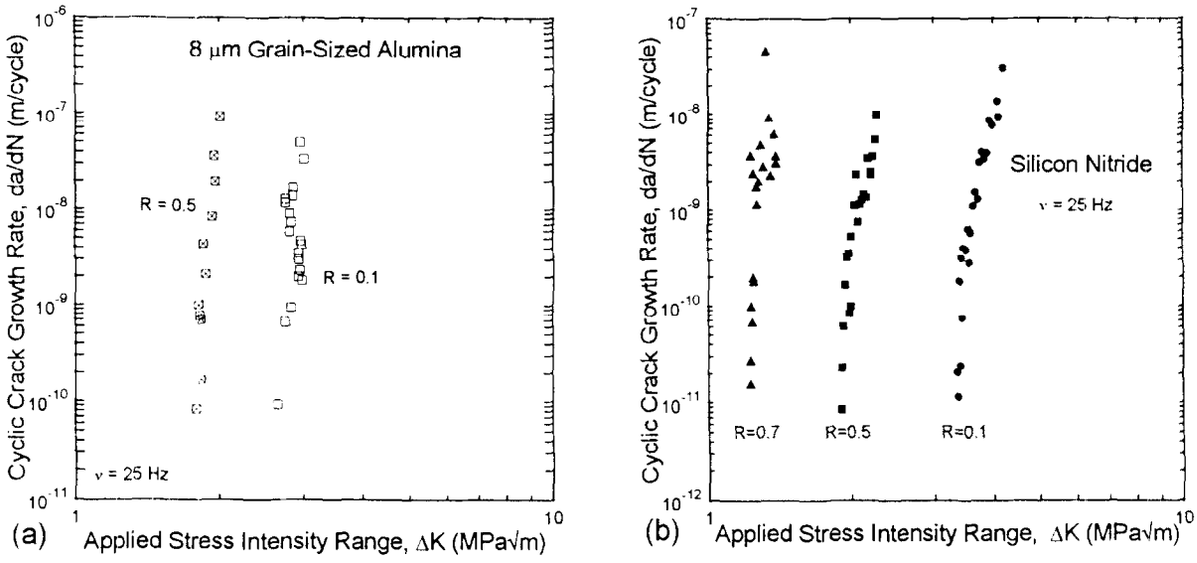

Fig. 7. Effect of load ratio on crack growth-rate behaviour, plotted in terms of ΔK.

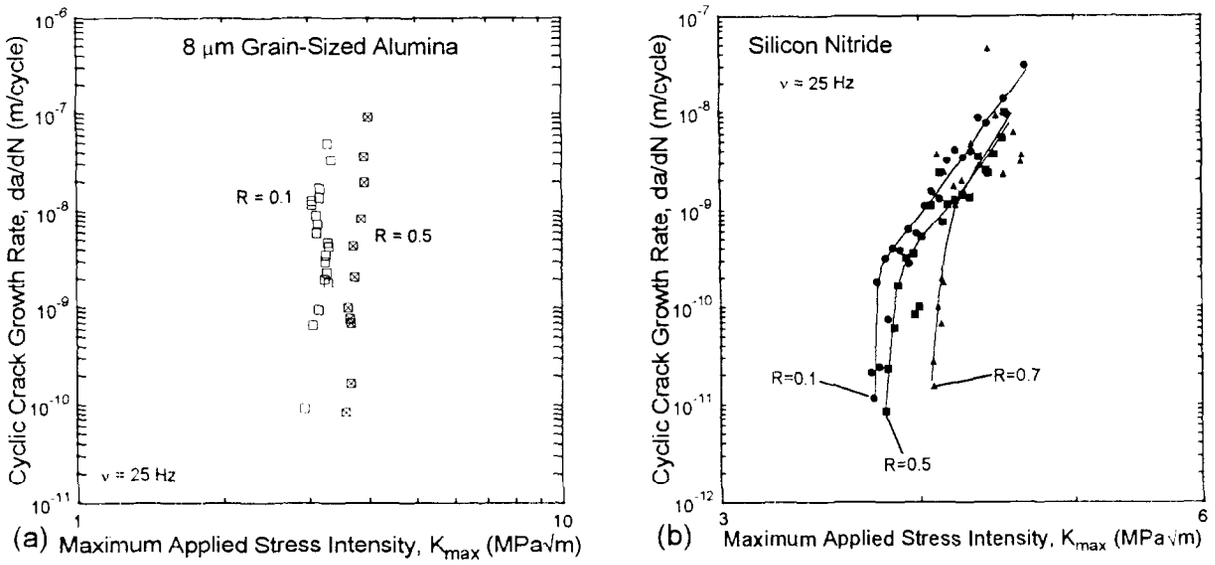

Fig. 8. Effect of load ratio on crack growth-rate behaviour, plotted in terms of K_{max}.

Growth rates are accelerated with increasing load ratio, R, when plotted in terms of ΔK for both the 8 μm grain-sized Al_2O_3 and the Si_3N_4 (Fig. 7). Although the slope, m, is essentially unchanged, fatigue thresholds, ΔK_{th} (defined at 10^{-10} m/cycle), are decreased from ~2.3 $MPa\sqrt{m}$ at $R = 0.1$ to ~1.8 $MPa\sqrt{m}$ at $R = 0.5$ for the Al_2O_3, and from ~3.4 at $R = 0.1$ to ~1.9 at $R = 0.5$ to ~1.2 at $R = 0.7$ for the Si_3N_4. This variation in ΔK_{th} with R can be normalized by plotting growth-rate data as a function of K_{max} (Fig. 8). In fact, when written in terms of both K_{max} and ΔK, the crack growth "law", $da/dN = C'(K_{max})^p(\Delta K)^p$ [$C' = C(1 - R)^n$ and $(n + p) = m$], shows that unlike metals, ceramics display a far greater dependence on K_{max} than K. A fit to the data in Fig. 8 yields values for Al_2O_3 of $n \sim 21.8$ and $p \sim 9.8$, and for Si_3N_4 $n \sim 29$ and $p \sim 1.3$; by comparison, values for a Ni-based superalloy are $n \sim 0.4$ and $p \sim 3$.[11] Such observations that growth rates show a marked dependence on K_{max} and that grain-size effects can be normalized by plotting in terms of K_{max}/K_c^3 are consistent with the idea that the crack-advance mechanisms are similar for cyclic and static fatigue (though behaviour behind the crack tip is quite different).

By plotting growth rates in terms of K_{max} (Fig. 8), there is an apparent negative effect of load ratio (growth rates are accelerated with decreasing R at constant K_{max}). While this is observed in Si_3N_4 only at low growth rates, the effect is apparent over the entire range of growth rates in alumina. Such an effect is anticipated by considering that higher

load ratios (at constant K_{max}) result in a reduced sliding distance and therefore less boundary wear per loading cycle. The convergence of the Si_3N_4 data at high growth rates, however, reflects an increased dependence on K_{max}; in this instance, crack growth is dominated by events ahead rather than in the wake of the crack tip.

4 SUMMARY AND CONCLUSIONS

Fractographic and *in situ* crack-path analyses and the observed dependence of cyclic-crack growth rates on load ratio and grain size are found to be consistent with a cyclic fatigue mechanism in grain-bridging ceramics based on the degradation of a crack-tip shielding zone because of wear at the grain/matrix interface. Cyclic fatigue crack-growth rates are accelerated in finer-grained microstructures; this is attributed primarily to the diminished toughness. Growth rates are lowered, however, by increasing the load ratio at constant, K_{max}; this can be attributed to the reduction in the bridge/matrix sliding distance at high R values.

ACKNOWLEDGEMENTS

This work was supported by the U.S. National Science Foundation under Grant No. DMR-9123279. Thanks are due to Dr B. J. Dalgleish for his assistance with the microscopy and Dr R. W. Steinbrech for provision of the alumina.

REFERENCES

1. DAUSKARDT, R. H., A frictional-wear mechanism for fatigue-crack growth in grain-bridging ceramics. *Acta Metall. Mater.*, **41** (1993) 2765.
2. LATHABAI, S., RÖDEL, J. & LAWN, B., Cyclic fatigue from frictional degradation at bridging grains in alumina. *J. Am. Ceram. Soc.*, **74** (1991) 1340.
3. GILBERT, C. J., DAUSKARDT, R. H., STEINBRECH, R. W., PETRANY, R. N. & RITCHIE, R. O., Cyclic fatigue in alumina: Mechanisms of crack advance promoted by frictional wear of grain bridges. *J. Mater. Sci.*, **30** (1995) 643.
4. GILBERT, C. J., DAUSKARDT, R. H. & RITCHIE, R. O., Behaviour of cyclic fatigue cracks in monolithic silicon nitride. *J. Am. Ceram. Soc.*, **78** (1995) 2291.
5. DAUSKARDT, R. H. & RITCHIE, R. O., Cyclic fatigue-crack growth behaviour in ceramics. *Closed Loop*, **17** (1989) 7.
6. OKAZAKI, M., McEVILY, A. J. & TANAKA, T., On the mechanism of fatigue crack growth in silicon nitride. *Metall. Trans.*, **22A** (1991) 1425.
7. KISHIMOTO, H., UENO, A., KAWAMOTO, H. & HUJII, Y., The influence of wave form and compressive loads on the crack propagation behaviour of a sintered Si_3N_4 under cyclic loads. *J. Soc. Mater. Sci. Jpn*, **38** (1989) 1212.
8. EVANS, A. G. & McMEEKING, R. M., On the toughening of ceramics by strong reinforcements. *Acta Metall. Mater.*, **34** (1986) 2435.
9. VEKINIS, G., ASHBY, M. F. & BEAUMONT, P. W. R., R-curve behaviour of alumina ceramics. *Acta Metall.*, **38** (1990) 1151.
10. ESHELBY, J. D., The determination of the elastic field of an ellipsoidal inclusion and related problems. *Proc. R. Soc. Lond.*, **A241** (1957) 376.
11. VAN STONE, R. H., Residual life prediction methods for gas turbine components. *Mater. Sci. Eng.*, **A103** (1988) 49.